Proceedings of the 20th International Conference on Soil Mechanics and Geotechnical Engineering– Rahman and Jaksa (Eds)

Numerical analysis of deep ground movements induced by circular shaft construction

Analyse numérique des mouvements profonds du sol induits par la construction de puits circulaires

Emilio Bilotta, Nicola De Falco
Department of Civil, Architectural and Environmental Engineering, University of Napoli Federico II, Naples, Italy.

Sam Divall
Department of Civil Engineering, City, University of London, UK.

Richard Goodey
School of Engineering and the Environment, Kingston University London, UK

ABSTRACT: The prediction of the excavation-induced displacements by shaft construction in urban areas is an important design issue. A series of experiments were conducted by Le et al. (2019) using a geotechnical centrifuge to evaluate the distribution with depth of soil movements induced during a shaft construction. Those results have been confirmed and expanded in this work by means of numerical analyses. Following this validation, numerical modelling has been used to analyse the influence of OCR and of the shaft geometry, namely its depth H and diameter D_{shaft}. In the abovementioned experimental study (Le et al., 2019) the presence of existing underground structures in the proximity of the shaft had been neglected. Therefore, in this study the effect of an existing shallow tunnel in the vicinity of the shaft excavation was taken into account and numerically analysed. The results show that the induced displacement field is affected by the tunnel, depending on its distance from the shaft. Nevertheless, when the distance between the shaft and the existing tunnel is larger than the tunnel axis depth, the tunnel presence may be neglected in the prediction of shaft-indued displacements. Based on the numerical results, further centrifuge tests will be carried out to model the interaction between the shaft excavation and the tunnel.

RÉSUMÉ: La prévision des déplacements induits par l'excavation par la construction de puits dans les zones urbaines est une question de conception importante. Une série d'expériences ont été menées par Le et al. (2019) à l'aide d'une centrifugeuse géotechnique pour évaluer la distribution avec la profondeur des mouvements du sol induits lors de la construction d'un puits. Ces résultats ont été confirmés et étendus dans ce travail au moyen d'une analyse numérique. Suite à cette validation, une modélisation numérique a été utilisée pour analyser l'influence de l'OCR et de la géométrie de l'arbre, à savoir sa profondeur H et son diamètre D_{shaft}. Dans l'étude expérimentale susmentionnée (Le et al., 2019), la présence de structures souterraines existantes à proximité du puits avait été négligée. Par conséquent, dans cette étude, l'effet d'un tunnel peu profond existant à proximité de l'excavation du puits a été pris en compte et analysé numériquement. Les résultats montrent que le champ de déplacement induit est affecté par le tunnel, en fonction de sa distance par rapport au puits. Néanmoins, lorsque la distance entre le puits et le tunnel existant est supérieure à la profondeur de l'axe du tunnel, la présence du tunnel peut être négligée dans la prédiction des déplacements induits par le puits. Sur la base des résultats numériques, d'autres essais par centrifugation seront effectués pour modéliser l'interaction entre l'excavation du puits et le tunnel.

KEYWORDS: ground movements, shaft, tunnel, deep excavation, numerical validation

1 INTRODUCTION

The rapid development of modern cities has led to a lack of surface space. In response to this, the use of underground space provides an ideal location for hosting infrastructure. The most obvious example is that of tunnels, which are widely used for connections in transport systems, water services, sewerage, communications networks and power lines. In congested metropolitan environments, the main obstacle to the exploitation of underground space is the means of access: vertical shafts have been mostly used in recent years due to their lower footprint requirement. Their relatively straightforward construction, as well as their larger stiffness compared with other supported open excavations, makes shafts particularly suitable in situations of restricted space or unfavourable ground conditions. On the other hand, since shaft construction is commonly carried out near existing buildings or other underground structures (such as deep foundations or tunnels), the prediction at the design stage of the potential ground movements is very important.

The displacement field induced by shaft excavation is mainly due to the reduction of the radial state of stress on the shaft sides and of the vertical stress at the bottom. Additional displacements can arise due to variation of the groundwater level and, in fine-grained soils, due to consolidation. Empirical methods are usually adopted for a rapid assessment of ground movements induced by shaft construction, based on monitoring data from construction sites.

Even though shaft construction techniques utilised in urban environments have rapidly evolved in recent years and shafts are more regularly being constructed, available on-site measurement data is relatively scarce in the literature. New (2017), extending a previous relationship proposed by New & Bowers (1994), provided a method that allows the surface settlements to be predicted as a function of the shaft depth, *H*, and of the distance, *d*, from the internal lining:

$$s_v^{surface} = \alpha H(1 - d/nH)^2 \quad (1)$$

This equation needs two parameters to be calibrated: *n*, identifying the distance at which the vertical displacements at

ground surface is negligible, and α, which takes into account the excavation method and the soil conditions. New (2017) acknowledges that these parameters are likely to be calibrated based on previous site measurements.

Le et al. (2019) conducted physical modelling of shaft excavation in clay, using the centrifuge facility at City, University of London, to investigate the sub-surface displacement profiles at different distances, d, from the shaft lining. The distributions of the displacement profiles obtained in the testing represents quite well the data from site measurements reported by different authors (Wong & Kaiser, 1988; McNamara et al., 2008; Schwamb et al., 2016). Near the shaft, the vertical displacements exhibit a *parabolic* shape, the horizontal ones a *Gaussian* shape. Based on this, a procedure for estimating ground movements was proposed by Le et al. (2019) and is summarised in Figure 1. The dataset of displacement measurements resulting from that study can be used, together with the data collected in the field by other researchers, as a reference for validating numerical modelling.

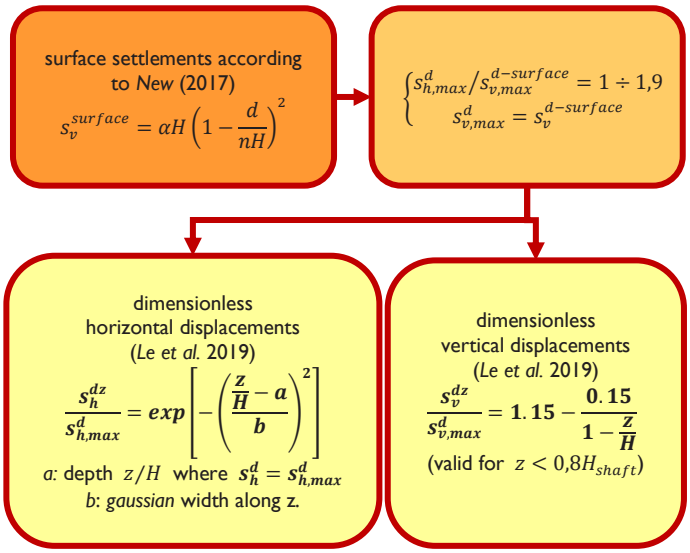

Figure 1. Prediction procedure proposed by Le et al. (2019).

In this work, a numerical back-analysis of a reference centrifuge test has been carried out. It is analysed with the aim of verifying the ability to reproduce numerically the experimental results. The final purpose is that of validating a numerical model to extend the scope of the study and more details of this process are given in De Falco (2020). Using the validated numerical model, a parametric analysis was carried out varying the geometric and mechanical conditions from those of the centrifuge reference case. The effects of different excavation depth and diameter as well as those of different overconsolidation ratios have been explored. Finally, the interaction between the pre-existing displacement field due to the presence of a tunnel nearby and that caused by the excavation of the shaft was studied.

2 NUMERICAL MODELING

2.1 *Methodology*

The centrifuge test procedure was modelled at the prototype scale by using the finite element code Plaxis 3D (Brinkgreve et al., 2018). Three groups of calculation phases can be distinguished (Figure 2): (a) consolidation; (b) pre-excavation; (c) excavation.

During the consolidation phase (Fig. 2a), the Speswhite kaolin used in the centrifuge test is overconsolidated through a uniform vertical loading up to 500kPa, before undergoing the gravity stress profile, to reproduce test CR500 carried out by Le et al. (2019). Prior to the excavation (Fig. 2b), the *excavation support system* is installed in the physical model – before it is moved to the centrifuge swing. It consists of a cylindrical liner and a basement that prevent soil movements while removing the soil inside. This phase, that is performed very quickly in the experiments, is modelled in undrained conditions, by activating very rigid elements (dimensions are shown in Figure 2b) and removing the clay elements inside.

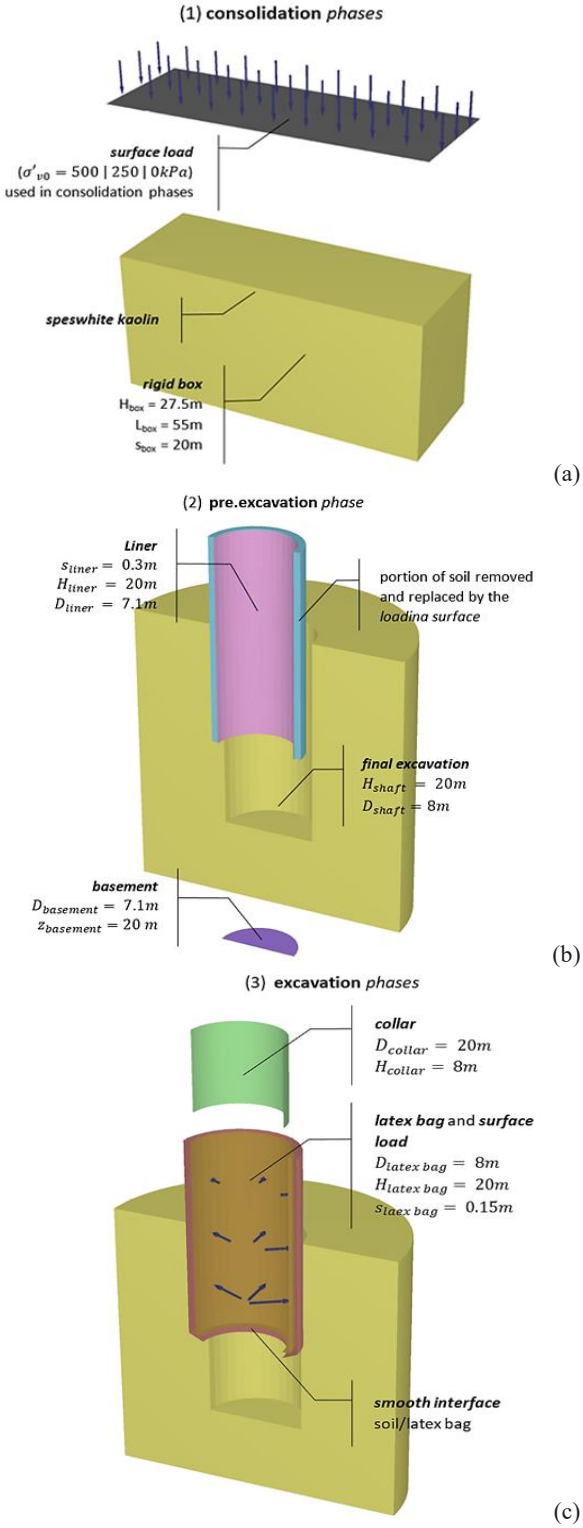

Figure 2. Staged construction phases if FEM numerical models: a) consolidation; b) pre-installation; c) excavation.

During the centrifuge flight, the shaft excavation is simulated by draining a latex bag located in the interspace between the liner and the cavity wall. This contains a heavy fluid (sodium polytungstate) with a specific weight close to the unit weight of clay, which serves to simulate the lithostatic conditions prior to excavation. In numerical modelling, the supporting effect of the fluid pressure is modelled by a horizontal radial load linear increasing with z. This load is reduced to zero to simulate the fluid drainage in the centrifuge and, therefore, the excavation. In addition, a latex collar is simulated in the cavity (Figure 2c) to reproduce a further stiffening effect provided in centrifuge by the latex bag (E= 5 MPa, ν=0.5). In fact, in the centrifuge tests the latex bag is connected, on the surface, to an aluminum ring even during the fluid drainage. Thickness and height of the collar were defined through a back-analysis, taking as target the surface displacement in the centrifuge test.

Hardening soil with small strain overlay (Schanz et al., 1999; Benz et al., 2009) was used as a material model for clay. It is an elastic–plastic model with isotropic hardening, which is able to account for the non-linear strain dependency of stiffness from very small strain to higher strain level. The constitutive parameters were calibrated on the results of Benz (2007) and they are shown in Table 1.

Table 1. HSss model parameters for Speswhite kaolin

Parameters	*Value*
γ_{sat} unsaturated unit weight	17 kN/m^3
G_0^{ref} *Small-Strain* stiffness	33300 kN/m^2
$\gamma_{0,7}$ shear strain @ $0{,}7G_0$	2×10^{-4}
ν'_{ur} Poisson's ratio	0.35
E_{50}^{ref} triaxial compression stiffness	1500 kN/m^2
E_{50}^{ref} primary oedometer stiffness	750 kN/m^2
E_{ur}^{ref} unloading/reloading stiffness	8000 kN/m^2
c cohesion	≈0 kN/m^2
φ friction angle	21°

The decay of kaolin shear stiffness with the strain level is validated in Figure 3 by comparing the numerical prediction of the behaviour of single element along drained triaxial path (p'=300 kPa) with the results of drained triaxial tests on reconstituted kaolinite clay at confining pressure of 300kPa (from Benz, 2007).

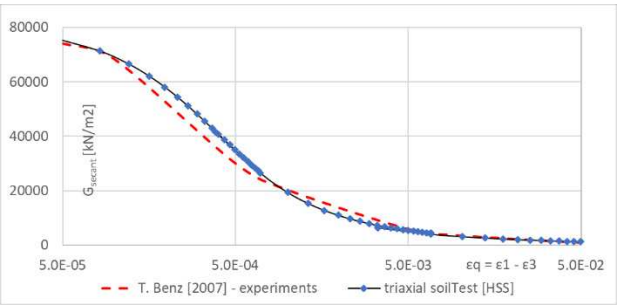

Figure 3. Comparison between single element prediction of shear modulus decay and experimental results from triaxial tests after Benz (2007).

2.2 *Results of back-analysis*

Confirming the test observations, the largest displacements occur at the shaft wall, in horizontal direction at a depth of about $0.6H_{shaft}$. The displacements are completely exhausted at a distance of $1.5H_{shaft}$ from the lateral surface of the shaft, that is d = 30 m. Figure 4 shows the profiles with depth of the horizontal and vertical components of displacement at different distances, d, from the excavation wall. The displacement profiles have been made non-dimensional by dividing them by the maximum values of horizontal and vertical displacement, respectively. Until $d/H < 0.4$ the vertical displacements show the expected parabolic distribution while the horizontal displacement profiles display a Gaussian distribution (Le et al., 2019). The design non-dimensional profiles proposed by Le et al. (2019) are shown in the figure for comparison.

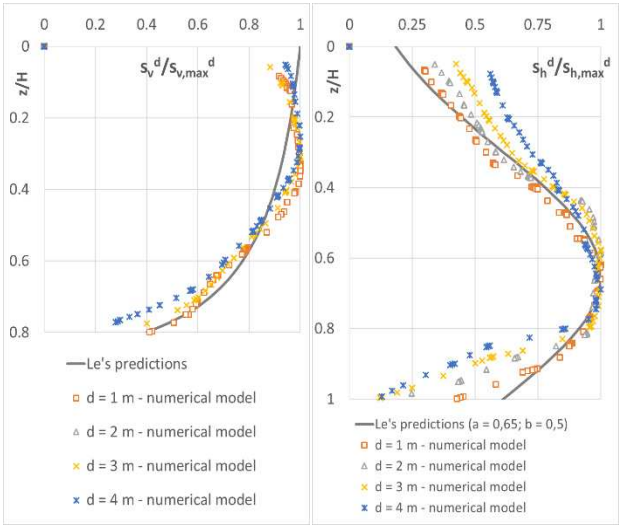

Figure 4. Non-dimensional horizontal (b) and vertical (c) displacement profiles computed at varying d and comparison with Le et al. (2019).

Figure 5 compares the calculated settlement trough with the centrifuge test results (Le et al., 2019) and prediction using Equation (1) of New (2017). Values of n=1 and α=0.0025 were assumed in order to obtain the best fitting of Eq. (1) to the numerical model results. Using the parameters estimated by Le et al. (2019) on the back analysis of field data from Wong & Kaiser (1988), a different surface settlement curve would be obtained, due to the different boundary conditions occurring in the field. Hence, suitable conditions must be considered to apply the predictive procedure proposed by Le et al. (2019), such as those depending on the excavation method and the initial conditions of the soil (OCR). In the following section 3 the influence of OCR and of shape ratio D_{shaft}/H_{shaft} is taken into account.

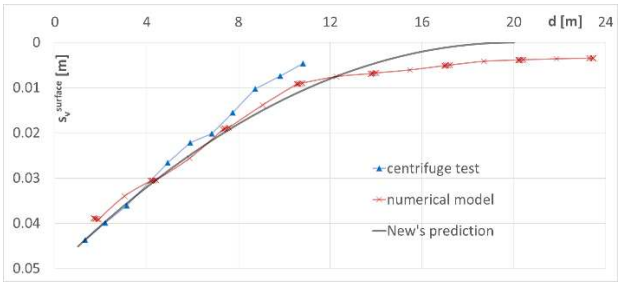

Figure 5. Computed settlement trough compared with centrifuge test results (Le et al., 2019) and New (2017) prediction (Eq.1, α=0.0025, n=1).

3 PARAMETRIC ANALYSIS

Once the numerical model was validated against the results of centrifuge tests, it was used to extend the scope of the study. The influence of ground conditions and shaft geometry was investigated by varying the overconsolidation ratio (OCR) of the clay and the size of the excavation. Furthermore, the presence of a tunnel close to the shaft was considered, to explore the limit of applicability of the existing solutions in congested urban

underground. The results of parametric analyses are shown in the following sections.

Table 2. Index of cases studied in parametric analysis

ID Case	D_{shaft}	H_{shaft}	σ'_{v0}
Reference Case 1	8m	20 m	500 kPa
Case 2.a	8m	20 m	750 kPa
Case 2.b	8m	20 m	350 kPa
Case 3	10m	20 m	500 kPa
Case 4	8m	16 m	500 kPa
Shaft/tunnel Interaction Cases	*Case 5*	$d_{tunnel} = 6\ m$	
	Case 6	$d_{tunnel} = 8\ m$	
	Case 7	$d_{tunnel} = 12\ m$	

3.1 *Influence of OCR*

The influence of OCR has been investigated with the same geometrical model by changing the maximum value of the over-consolidation stress, σ'_{vP}, before excavation (cf. Table 2). The uniform vertical loading (see §2.1) was set to 750 kPa (case 2) and 350 kPa (case 3). This variation determines a change in the OCR profile and therefore in the initial stress state. Figure 6 clearly shows the stiffening of the material and a reduction in the magnitude of displacements. However, the dimensionless profile of displacements is not affected by the different initial conditions and well matches the distribution by Le et al. (2019).

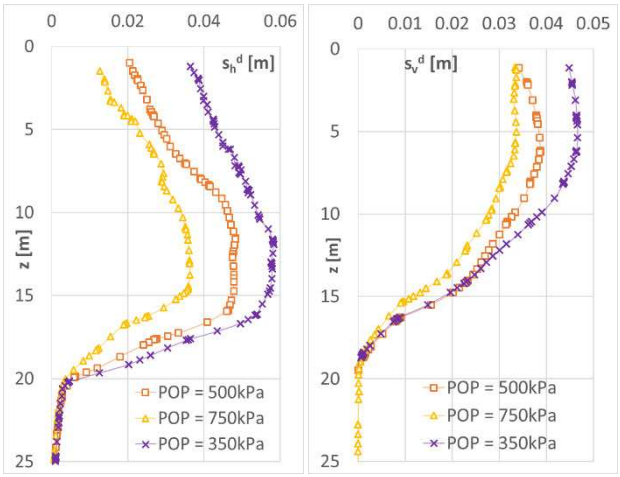

(a) (b)

Figure 6. Influence of σ'_{vP} on horizontal (b) and vertical (a) displacement at d=3m.

The coefficient α of Eq. (1) can be therefore adjusted to take into account the influence of overconsolidation ratio evaluated at the maximum depth of the domain in the numerical model ($z = 27.5\ m$). Using the results of the numerical analyses the value of α has been back-calculated and a linear dependency on OCR has been found (Figure 7) as $\alpha = m \cdot OCR + q$.

This equation can be used to assess the surface settlement through, extending to different values of OCR the validity of Le et al. (2019) procedure to predict ground movements around the shaft. However, for practical applications it should be generalized to different soils and excavation methods.

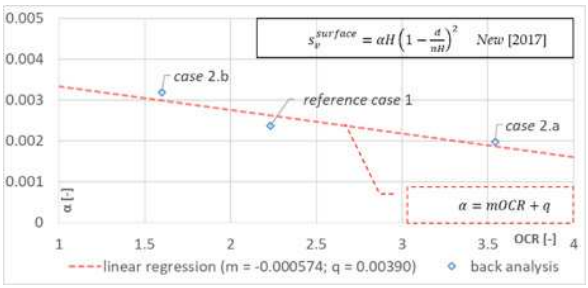

Figure 7. Coefficient α in Eq. 1 as a function of OCR.

3.2 *Influence of shaft geometry*

The influence of shaft geometry has been investigated in analyses 4 and 5, both in the same initial conditions as the reference case 1. Compared to case 1, in case 4 the excavation diameter was increased ($D_{shaft} = 10\ m$), in case 5 its depth was reduced ($H_{shaft} = 16\ m$). Figure 8 shows a comparison among the displacement profiles in the three cases.

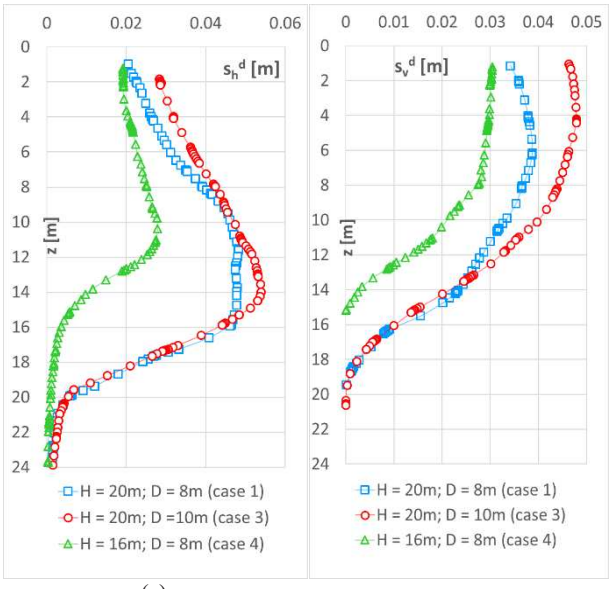

(a) (b)

Figure 8. Influence of shaft geometry: comparison between profiles of horizontal (a) and vertical displacements (b) at d=3m in cases 4, 5 and in the reference case 1.

Increasing the shaft diameter slightly increases the ground movements (case 3 *vs.* case 1). This is mainly due to the larger volume of soil that is affected by bottom heave, in undrained conditions. This issue is not taken into account in the procedure by Le et. al (2019). On the other hand, the reduction of the excavation depth causes a large reduction of the ground movements at the sides (case 4 *vs.* case 1), that is also somehow expected. The procedure by Le et al. (2019) is able to take into account such a variation, by changing parameters a and b. It is also worth noting that, despite the ratio H_{shaft}/D_{shaft} is the same in case 3 and 4, the resulting displacements are very different.

3.3 *Interaction with an existing tunnel*

The effect of the presence of adjacent tunnel (D_{tun}=8m, C_{tun}/D_{tun}=1) on the ground movements induced by the shaft excavation has been studied according to the geometrical sketch in Figure 9 (case 5).

In *shaft/tunnel interaction case* the tunnel is modelled – as often occurs in centrifuge tests – as a circular cavity supported by a latex membrane with a heavy fluid filling the gap between the membrane and a rigid liner (Williamson, 2014). The excavation is then simulated through the removal of the heavy

fluid from inside the cavity. In numerical modelling the process is divided in phases, similar to the shaft excavation above described. Since the tunnel is assumed to be pre-existing to the shaft, first the heavy fluid is removed from the tunnel (in the *tunnelling phase*) and then from the shaft (*shaft-excavation phase*). Tunnel excavation is carried out in drained conditions, thus simulating long term. Hence, tunnel excavation produces different ground conditions before the excavation of the shaft. Figure 10 shows a comparison between two profiles of displacements with depth at a distance d=3 m from the shaft. They were computed in case 1 (reference case, without tunnel) and in case 5. In both cases the displacements are only caused by the shaft excavation (any displacement calculated in previous calculation stages is subtracted).

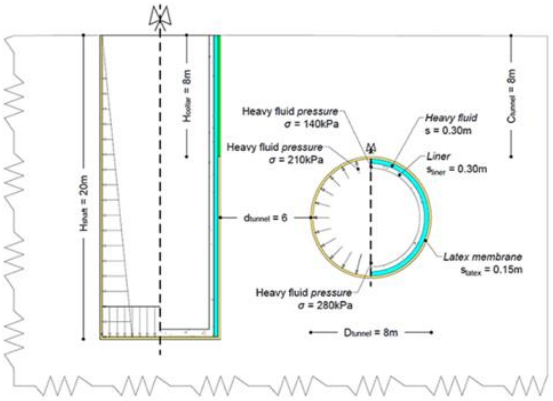

Figure 9. Geometry of the interaction problem shaft/tunnel (case 5).

It can be observed that the horizontal displacements induced by the shaft excavation are different in the two cases, being larger in the latter (case 5). At the tunnel axis depth (12 m) the difference attains a maximum, indicating a lower soil stiffness, produced by the shear deformation induced by the previous tunnelling operations.

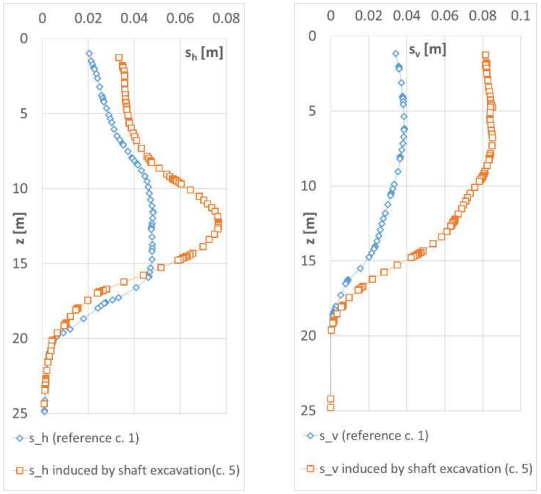

(a) (b)

Figure 10. Interaction with an existing tunnel: horizontal (a) and vertical (b) displacements caused by the shaft excavation after tunnelling (case 5) compared to those of the reference case 1 (d= 3m).

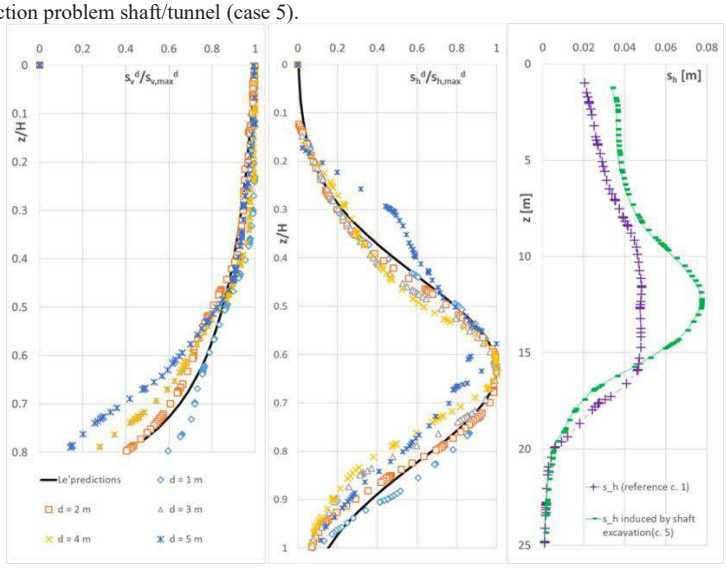

(a) (b) (c)

Figure 11. Influence of existing tunnel on displacements caused by shaft excavation (c), vertical (a) and horizontal (b) dimensionless displacements in case 5.

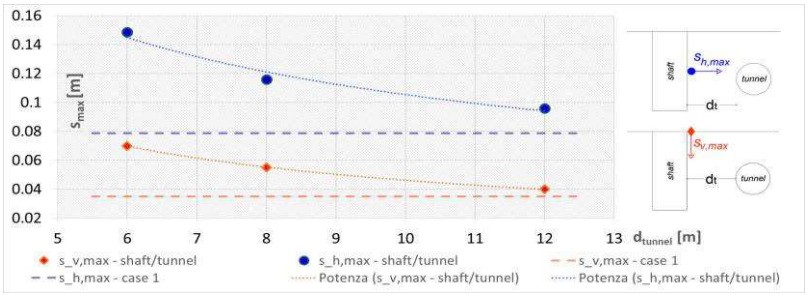

Figure 12. Influence of the net distance d_{tunnel} in the shaft/tunnel interaction problem.

The interference with the pre-existing tunnel is even clearer from the dimensionless displacement profiles in Figure 11. Lateral movements (Fig. 11b) tend to diverge from the typical Gaussian shape approaching the tunnel spring lines (d=5m). Nevertheless, near the shaft it would still be possible to use Le et al. (2019) equations, provided that the right value of settlement trough is used, that takes into account this interaction. Interaction reduces by increasing the distance between the tunnel and the shaft (d_{tunnel}).

The limit distance in this case is 12 m and it can be observed in Figure 12, where the results of case 6 ($d_{tunnel} = 8\ m$) and of case 7 ($d_{tunnel} = 12\ m$) are compared to those of case 5 ($d_{tunnel} = 6\ m$) and of the reference case 1 (no tunnel). In case 7 the profile of displacements near the shaft tends to that in the reference case 1. In fact, it is evident from the plot that with increasing d_{tunnel}, both the vertical and the maximum horizontal displacement near the shaft tend to the corresponding values of the reference case in which the tunnel is absent.

4 CONCLUSIONS

The analysis of the centrifuge test series conducted by Le et al. (2019) at City, University of London highlighted the importance of accurate vertical and horizontal displacement prediction. Potentially, at the design stage the procedure summarised in Figure 1 allows to obtain dimensionless displacement profiles very close to the results of physical models and field monitoring. Clearly, by expanding the test dataset upon which the procedure has been calibrated, it would be possible to better predict the displacements expected on site in different conditions. This implies diversifying ground conditions (e.g. further changing the previous stress history or the type of soil) or shaft geometry in the centrifuge tests. However, some differences may occur due to the influence of details of the construction procedure on the displacement field.

Numerical modelling may help to explore a larger variability in the input data. Using appropriate constitutive laws, numerical modelling takes advantage of the results of centrifuge tests by careful calibration of parameters and validation of the model.
In this work a numerical model was elaborated to simulate the centrifuge tests by Le et al. (2019) on shaft excavation in clay. The calculated profiles of the displacements well reproduced the experimental results.

Numerical modelling also shows that the assessment procedure by Le et al. (2019) may be used to realistically assess the ground displacement around the shaft, provided that the equation calculating the surface settlement trough (New, 2017) is adapted to the appropriate conditions. In fact, a parametric analysis was carried out by varying the maximum overconsolidation stress and the shaft geometry.

The results of the analyses were used to determine the dependence of the parameter α of New (2017) from OCR, confirming that this parameter, in addition to being dependent on the construction method of the shaft, strongly depends also on the initial conditions of the soil. Influencing the estimation of the surface settlement, the coefficient α inevitably affects the entire prediction procedure for underground displacements. This result will be the starting point of a more in-depth experimental study on the dependence of the empirical parameters on the initial conditions of the soil.

The influence of the excavation depth, *H*, on the deformation field is implicitly taken into account in the proposed formulations, and this has been verified in the numerical results. Furthermore, it has been shown that the excavation width influences the magnitude of displacements, although it is not taken into account explicitly in the predictive procedure. Hence the influence of excavation diameter D_{shaft} may deserve further experimental investigation.

Finally, the numerical analysis of tunnel/shaft interaction has shown how the preceding tunnel construction may alter the ground conditions prior the shaft excavation, hence the ground displacements that the latter induces. The procedure by Le et al. (2019) may still be used in this case, by accepting some discrepancy between the predicted and the observed profiles. However, if the shaft is excavated at a distance from the tunnel lower than the tunnel axis depth, that procedure may easily underestimate the maximum values of horizontal and vertical displacement by a factor of two.

5 ACKNOWLEDGEMENTS

The authors gratefully acknowledge the support of the Leverhulme Trust grant no. RPG-2013-85.

6 REFERENCES

Benz T. (2007). Small-Strain Stiffness of Soils and its Numerical Consequences (PhD thesis), Universität Stuttgart, Germany.

Benz T., Schwab R., & Vermer P. (2009). Small-strain stiffness in *geotechnical analyses*.

De Falco. (2020). Back-analysis of centrifuge modelling of a shaft excavation in urban area - University of Naples Federico II, Naples, Italy (in Italian).

Divall S. & Goodey R. J. (2016). An apparatus for centrifuge modelling of a shaft construction in clay, 3rd European Conference on Physical Modelling in Geotechnics (*Eurofuge 2016*) 1-3 June, Ifsttar, Nantes, France.

Kappert M. H. & Bonnier P. G. (2007). Hysteretic damping in a small-strain stiffness model, NUMOG X.

Le B. T., Goodey R. J. & Divall S. (2019). Subsurface ground movements due to circular shaft construction, *Soils and Foundations*, Vol. 59, No. 5, pp. 1160–1171.

McNamara A., Roberts T., Morrison P. & Holmes G. (2008). Construction of a deep shaft for Crossrail. In: *Proc. Instn Civ. Engrs Geotech. Engng*, vol. 161, pp. 299–309.

New B. (2017). Settlements due to shaft construction. In: Tunnels and Tunnelling International, September 2017, pp 16-17.

New B. (2017). Settlements due to shaft construction. In: Tunnels and Tunnelling International, September 2017, pp 16-17.

New B. & Bowers K. (1994). Ground movement validation at the heathrow Express trial tunnel, *Tunnelling '94 Proc. 7th Int. Symp. IMM* and *BTS. Chapman and Hall*, London, pp. 301-329.

Schwamb T., Soga K., Elshafie M.Z.E.B. & Mair R.J. (2016). Considerations for monitoring of deep circular excavations - *Proc. Instn Civ. Engrs Geotech. Eng.* 169 (6), 477–493.

Shanz T., Vermer P.A. & Bonnier P.G. (1999). Beyond 2000 in *Computational Geotechnics*, chapter Formulation and verification of The Hardening-Soil model, pages 281-290, Balkema, Rotterdam.

Williamson, M. G. (2014). Tunnelling effects on bored piles in clay, PhD Thesis, University of Cambridge, Cambridge, UK.

Wong R.C.K.R. & Kaiser P.P.K. (1988). Behaviour of vertical shafts: reevaluation of model test results and evaluation of field meadurements, Can. Geotech. J. 25(2), 338-352.

Zhang T., Taylor R. N., Divall S., Zheng G., Sun J., Stallebrass S. E. & Goodey R. J. (2019). Explanation for twin tunneling-induced surface settlements by changes in soil stiffness on account of stress history, *Tunnelling and Underground Space Technology*, Vol. 85, pp. 160–169.